View Article Online / Journal Homepage / Table of Contents for this issue

Journal of Materials Chemistry

www.rsc.org/materials

Volume 18 | Number 17 | 7 May 2008 | Pages 1937–2052

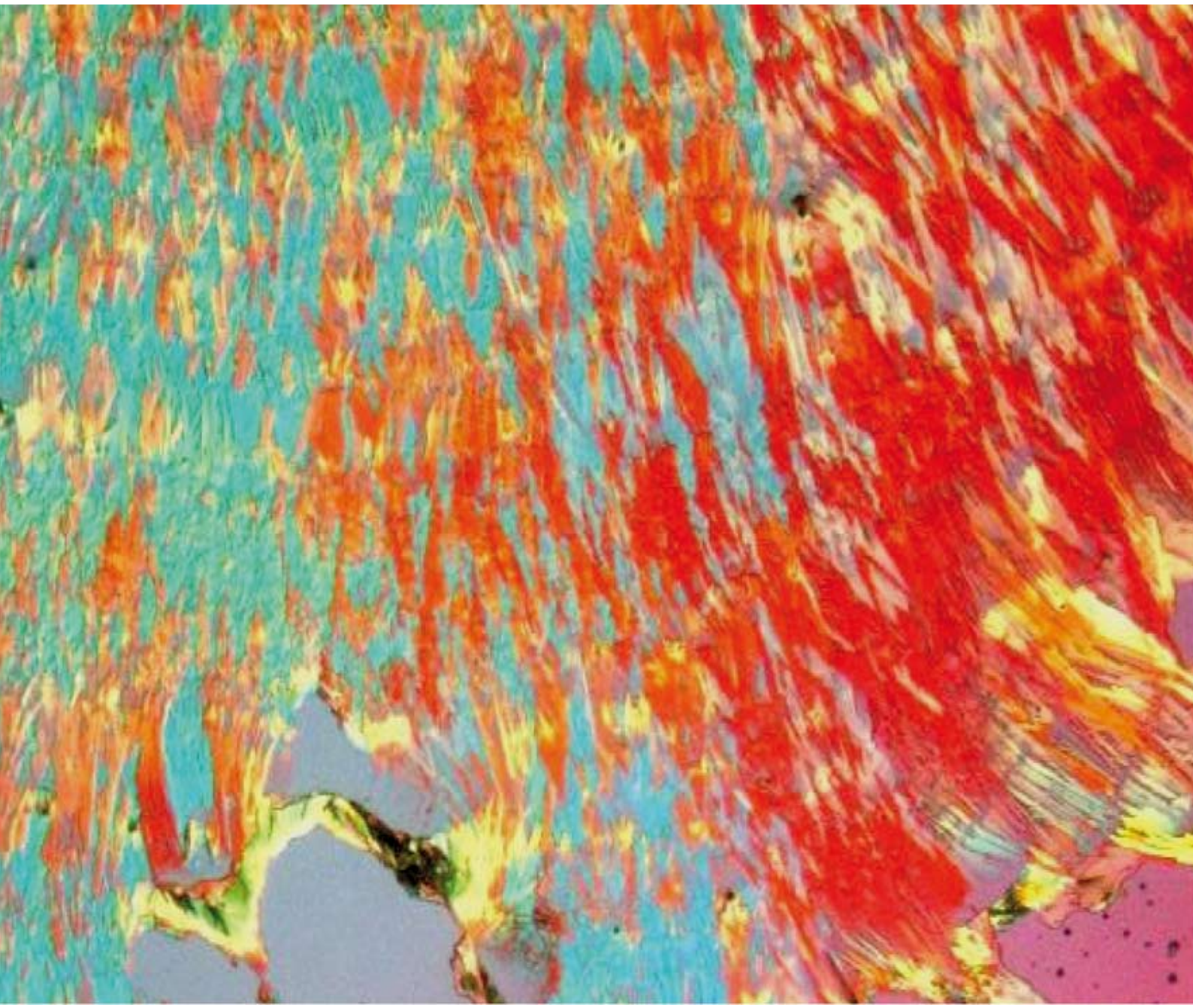

ISSN 0959-9428

RSC Publishing

0959-9428(2008)18:17;1-W

The influence of side chains on the structures and properties of functionalized pentacenes†‡

Jihua Chen,[ab] Sankar Subramanian,[d] Sean R. Parkin,[d] Maxime Siegler,[d] Kaitlin Gallup,[b] Chelsea Haughn,[b] David C. Martin*[abc] and John E. Anthony*[d]

Received 5th November 2007, Accepted 15th January 2008
First published as an Advance Article on the web 12th February 2008
DOI: 10.1039/b717082c

Published on 12 February 2008. Downloaded by CASE WESTERN RESERVE UNIVERSITY on 30/10/2014 17:04:20.

We investigated substituent-induced variations in microstructure and physical properties of a family of functionalized pentacenes, materials currently of intensive interest for making organic electronic devices such as thin film transistors, to shed light on the complex relationships between functionalization, film formation, stability, and microstructure. In this study, the pentacenes were modified with alkyl acetylene or alkylsilylethynyl groups with systematic variations in the alkyl chain length. With a proper side chain, this modification can effectively disrupt the herringbone packing seen in neat pentacene, promoting face-to-face arrangements between the acene rings and providing solubility in a variety of convenient solvents. Thin films can be readily formed by solution casting from THF, bromobenzene, toluene and other organic solvents. We have investigated the structure and properties of the functionalized pentacenes using UV-vis spectroscopy, hot stage optical microscopy, differential scanning calorimetry, transmission electron microscopy, X-ray and electron diffraction. The materials show regular variations in their thermal behavior, crystal packing and macroscopic properties as the chemistry of the side-group substituent changes.

1. Introduction

Molecular structure plays a central role in optimizing the performance of organic electronic devices such as solar cells, thin film transistors, and organic light emitting diodes,[1–10] with either organic small molecules or polymeric semiconductors.[11] For organic small molecules, extensive research has been done to study the effects of conjugation length and side chain type on device performance. In the case of oligoacenes in particular, conjugation length was found to have a close relationship with band gap (E_g), with a continuous decrease in gap observed as the number of acene rings increased from benzene to pentacene.[12] A similar trend was reported by Garnier *et al.* in oligothiophenes,[5,7,8] and Yanagi *et al.* in biphenyl oligothiophenes.[13] In addition, Garnier *et al.* pioneered the influence of α-, ω-, and β-substituted alkyl side groups on the microstructure and properties of sexi-thiophene.[5,7,8] The effect of side chain on charge carrier mobility has also been reported in a number of conjugated oligomer series, such as oligothienylenevinylenes,[14] and other oligothiophenes.[15–17] In general, proper side chains on the edge of the conjugated core units tended to improve the π–π interaction through alignment of the linear alkyl tails, thus improving mobility by often more than an order of magnitude; but at some critical length, it has been found that long-tail side groups began to occupy the spaces between aromatic planes, reducing the mobility of the films substantially.[5,7,8,14–17]

Through the past decade, pentacene made steady progress in the "mobility race" and has been studied extensively in various applications such as field-effect transistors,[18,19] circuits,[20,21] and paper-like electronic displays.[22–24] The key to extracting maximum performance from pentacene is to insure proper morphology of the thin films of this material, and since it has no appended alkyl groups to tune self-assembly, morphology is typically controlled by modification of the surface of the substrate,[25–27] which requires additional process steps. Other limitations with pentacene include poor solubility, which restricts its application in solution processes. In addition, pentacene molecules are known to adopt a herringbone structure in their polymorphs, limiting their π–π overlap.[28]

In this paper, we report the effect of systematic variation of side chains on the crystal packing, thin film morphology, thermal and optical properties of functionalized pentacenes. Functional groups in this study were either alkylethynyl or alkyl(diisopropylsilylethynyl) groups, with varying alkyl chain lengths. This chemical modification can effectively disrupt the herringbone packing of pentacene crystal, resulting in regular π–π stacking and giving solubility in a variety of organic solvents.

2. Experiments

2.1 Synthetic details

General. Solvents (acetone, methylene chloride, hexanes) were purchased from Fisher. Dry THF was either purchased from EM

[a]*Macromolecular Science and Engineering Center, The University of Michigan, Ann Arbor, Michigan, 48109, USA*
[b]*Department of Materials Science and Engineering, The University of Michigan, Ann Arbor, Michigan, 48109, USA*
[c]*Department of Biomedical Engineering, The University of Michigan, Ann Arbor, Michigan, 48109, USA. E-mail: milty@umich.edu*
[d]*Department of Chemistry, The University of Kentucky, Lexington, Kentucky, 40506, USA. E-mail: anthony@uky.edu*

† CCDC reference numbers 671507–671513. For crystallographic data in CIF or other electronic format see DOI: 10.1039/b717082c

‡ Electronic supplementary information (ESI) available: Detailed phase transition information extracted from DSC; UV-vis molar extinction coefficients; single crystal analysis. See DOI: 10.1039/b717082c

Published on 12 February 2008. Downloaded by CASE WESTERN RESERVE UNIVERSITY on 30/10/2014 17:04:20.

Science or distilled over sodium/benzophenone under N_2 atmosphere. Commercial acetylenes were purchased from GFS Chemicals. Silica gel 230–400 mesh was bought from Sorbent Technologies. NMR spectra were measured on Varian (Gemini 200 MHz/Unity 400 MHz) spectrometers, chemical shifts reported in ppm relative to $CDCl_3$ as internal standard. Mass spectroscopy was performed in EI mode at 70 eV or by MALDI with TCNQ matrix on a JEOL (JMS–700 T) Mass Spectrometer.

General procedure for the preparation of functionalized pentacenes. To an oven-dried 100 mL round-bottom flask containing the desired 1-alkyne (4.6 mmol) dissolved in 25 mL of dry THF (kept under a dry nitrogen environment) was added slowly n-BuLi (2.5 mmol), and this mixture was stirred for 40 min at room temperature. Then, 6,13-pentacenequinone (0.25 g, 0.8 mmol) was added quickly, and the mixture was stirred under a blanket of dry nitrogen overnight. Stannous chloride dihydrate (2 mmol) followed by 10% HCl (2 mL) were added to the reaction mixture which was stirred for an additional 7 h, after which it was extracted into hexanes, washed with saturated brine solution, dried over anhydrous $MgSO_4$ and concentrated. The crude products were purified by silica chromatography (typically using hexanes–methylene chloride (9 : 1 v : v)) and recrystallized from hexanes to yield pure materials.

6,13-Bis(hexynyl)pentacene (6-P). Yield = 0.28 g (80%), mp = 83 °C (decomp.). ^{1}H NMR (200 MHz, $CDCl_3$): δ 1.15 (t, J = 3.6 Hz, 6 H), 1.74–1.99 (m, 8 H), 2.95 (t, J = 3.4 Hz, 4 H), 7.39 (dd, J = 1.5 Hz, J = 3.3 Hz, 4 H), 8.01 (dd, J = 1.5 Hz, J = 3.2 Hz, 4 H), 9.18 (s, 4 H) ppm. ^{13}C NMR (50 MHz, $CDCl_3$): δ 13.93, 20.46, 25.52, 31.43, 79.11, 105.69, 118.52, 125.92, 126.34, 128.94, 130.73, 132.32 ppm. MS (EI 70 eV) m/z 438 (100%, M^+), 395 (35%, M^+ − propyl).

6,13-Bis(heptynyl)pentacene (7-P). Yield = 0.28 g (75%), mp = 115 °C. ^{1}H NMR (200 MHz, $CDCl_3$): δ 1.06 (t, J = 3.6 Hz, 6 H), 1.50–1.61 (m, 4 H), 1.7 (quintet, J = 3.5 Hz, 4 H), 1.97 (quintet, J = 3.5 Hz, 4 H), 2.94 (t, J = 3.4 Hz, 4 H), 7.39 (dd, J = 1.4 Hz, J = 3.4 Hz, 4 H), 8.01 (dd, J = 1.6 Hz, J = 3.2 Hz, 4 H), 9.20 (s, 4 H) ppm. ^{13}C NMR (50 MHz, $CDCl_3$): δ 14.31, 20.76, 22.57, 29.03, 31.66, 79.13, 105.78, 118.54, 125.94, 126.35, 128.93, 130.76,132.34 ppm. MS (EI 70 eV) m/z 466 (100%, M^+), 409 (20%, M^+ − butyl).

6,13-Bis(octynyl)pentacene (8-P). Yield = 0.25 g (62%). ^{1}H NMR (200 MHz, $CDCl_3$): δ 0.99 (t, J = 3.35 Hz, 6 H), 1.4–1.6 (m, 8 H), 1.77 (quintet, J = 3.3 Hz, 4 H), 1.96 (quintet, J = 3.53 Hz, 4 H), 2.95 (t, J = 3.4 Hz, 4 H), 7.39 (dd, J = 1.5 Hz, J = 3.35 Hz, 4 H), 8.01 (dd, J = 1.55 Hz, J = 3.3 Hz, 4 H), 9.21 (s, 4 H) ppm. ^{13}C NMR (50 MHz, $CDCl_3$): δ 14.30, 20.81, 22.92, 29.17, 29.33, 31.74, 79.13, 105.81, 115.59, 126, 126.42, 128.99, 130.82, 132.4 ppm. MS (EI 70 eV) m/z 494 (95%, M^+).

6,13-Bis(decynyl)pentacene (10-P). Yield = 0.25 g (56%). ^{1}H NMR (200 MHz, $CDCl_3$): δ 0.91 (t, J = 3.3 Hz, 6 H), 1.25–1.6 (m, 16 H), 1.77 (quintet, J = 3.55 Hz, 4 H), 1.96 (quintet, J = 3.53 Hz, 4 H), 2.94 (t, J = 3.5 Hz, 4 H), 7.39 (dd, J = 1.6 Hz, J = 3.4 Hz, 4 H), 8.02 (dd, J = 1.7 Hz, J = 3.3 Hz, 4 H), 9.20 (s, 4 H) ppm. ^{13}C NMR (50 MHz, $CDCl_3$): δ 14.23, 20.81, 22.88, 29.37, 29.52, 29.59, 32.11, 79.15, 105.8, 118.55, 125.91, 126.35, 128.93, 130.76, 132.33 ppm. MS (EI 70 eV) m/z 445 (25%), 429 (45%), 308 (100%).

6,13-Bis(dodecynyl)pentacene (12-P). Yield = 0.3 g (61%). ^{1}H NMR (200 MHz, $CDCl_3$): δ 0.87 (t, J = 3.3 Hz, 6 H), 1.20–1.60 (m, 24 H), 1.77 (quintet, J = 3.5 Hz, 4 H), 1.96 (quintet, J = 3.53 Hz, 4 H), 2.94 (t, J = 3.4 Hz, 4 H), 7.39 (dd, J = 5 Hz, J = 3.3 Hz, 4 H), 8.02 (dd, J = 1.5 Hz, J = 3.3 Hz, 4 H), 9.20 (s, 4 H) ppm. ^{13}C NMR (50 MHz, $CDCl_3$): δ 14.23, 20.81, 22.85, 29.37, 29.55, 29.87, 29.93, 32.09, 79.14, 105.79, 118.54, 125.91, 126.36, 128.94, 130.76, 132.33 ppm. MS (EI 70 eV) m/z 606 (20%, M^+), 479 (20%, M^+ − nonyl).

6,13-Bis(diisopropyl ethylsilylethynyl)pentacene (2-Si). Yield = 90%. ^{1}H NMR (200 MHz, $CDCl_3$): δ 0.90–1.10 (m, 4 H), 1.26–1.44 (m, 34 H), 7.43 (dd, J = 1.6 Hz, J = 3.4 Hz, 4 H), 8.00 (dd, J = 1.6 Hz, J = 3.3 Hz, 4 H), 9.31 (s, 4 H) ppm. ^{13}C NMR (50 MHz, $CDCl_3$): δ 2.55, 8.74, 12.18, 18.57, 18.86, 104.89, 107.51, 118.65, 126.32, 126.61, 128.99, 130.94, 132.64 ppm. MS (EI 70 eV) m/z 611 (56%, M^+).

6,13-Bis(diisopropyl n-butylsilylethynyl)pentacene (4-Si). Yield = 95%. ^{1}H NMR (200 MHz, $CDCl_3$): δ 0.96–1.04 (m, 8 H), 1.29–1.46 (m, 30 H), 1.50–1.60 (m, 4 H), 1.70–1.80 (m, 4 H), 8.00 (m, 4 H), 7.43 (m, 4 H), 9.31 (s, 4 H) ppm. ^{13}C NMR (50 MHz, $CDCl_3$): δ 10.28, 12.29, 14.10, 18.57, 18.84, 27.05, 27.28 104.64, 107.62, 118.46, 126.18, 126.44, 128.80, 130.75, 132.44 ppm. MS (EI 70 eV) m/z 667(65%, M^+), 610(20%, M^+ − butyl).

6,13-Bis(diisopropyl *sec*-butylsilylethynyl)pentacene (4II-Si). Yield = 88%.^{1}H NMR (200 MHz, $CDCl_3$): δ 1.2 (m, 8 H), 1.4 (m, 32 H), 1.58 (m, 4 H), 2.03–2.09 (m, 2 H), 7.44 (m, 4 H), 8.00 (m, 4 H), 9.32 (s, 4 H) ppm. ^{13}C NMR (50 MHz, $CDCl_3$): δ 11.89, 14.13, 14.95, 19.22, 19.15, 19.30, 19.54, 25.93, 104.94, 107.70, 118.58, 126.23, 126.53, 128.88, 130.85, 132.47 ppm. MS (EI 70 eV) m/z 667 (68%, M^+), 610 (20%, M^+ − *sec*-butyl).

6,13-Bis(diisopropyl hexylsilylethynyl)pentacene (6-Si). Yield = 91%. ^{1}H NMR (200 MHz, $CDCl_3$): δ 0.90 (m, 12 H), 1.35 (m, 38 H), 1.76 (m, 4 H), 7.45 (m, 4 H), 8.00 (m, 4 H), 9.30 (m, 4 H) ppm. ^{13}C NMR (50 MHz, $CDCl_3$): δ 10.68, 12.38, 14.38, 18.65, 18.92, 22.92, 25.11, 31.92, 33.90, 104.74, 107.71, 118.55, 126.22, 126.53, 128.89, 130.82, 132.50 ppm. MS (EI 70 eV) m/z 723 (68%, M^+), 638 (10%, M^+ − hexyl).

6,13-Bis(diisopropyl octylsilylethynyl)pentacene (8-Si). Yield = 85%. ^{1}H NMR (200 MHz, $CDCl_3$): δ 0.92(m, 10 H), 1.38 (m, 48 H), 1.77(m, 4 H), 7.43 (dd, J = 1.5 Hz, J = 3.3 Hz, 4 H), 8.00 (dd, J = 1.6 Hz, J = 3.3 Hz, 4 H), 9.30 (s, 4 H) ppm. ^{13}C NMR (50 MHz, $CDCl_3$): δ 10.71, 12.42, 14.29, 18.67, 18.94, 22.88, 25.19, 29.60, 29.70, 32.22, 34.26, 104.93, 107.85, 118.71, 126.36, 126.68, 129.05, 131.00, 132.69 ppm. MS (EI 70 eV) m/z 779 (68%, M^+), 666 (15%, M^+ − octyl).

2.2 UV-vis spectroscopy

A Cary 50-Bio UV Visible Spectrometer was used to examine THF solutions (30 ppm) of functionalized pentacenes.

 This journal is © The Royal Society of Chemistry 2008

Published on 12 February 2008. Downloaded by CASE WESTERN RESERVE UNIVERSITY on 30/10/2014 17:04:20.

Measurements were taken between wavelengths of 250 nm and 800 nm at medium speed.

2.3 Solution casting and thin film morphology

"Uncovered" and "covered" solution casting of functionalized pentacenes (from 0.1–0.2% wt. of THF, bromobenzene, or toluene solution) was performed on clean glass slides (as received from Fisher Scientific) or silicon wafers (cleaned as described elsewhere[29]) inside four-inch-diameter Petri dishes, either with or without cover on. A Spot RT Color 2.2.1 CCD camera (from Diagnostic Instruments, Inc.), and a Nikon OptiPhot2-POL optical microscope were used to take polarized optical micrographs.

Dilute THF solution droplets (0.1% wt.) of functionalized pentacenes were applied onto amorphous carbon thin films (20–50 nm) on copper grids (400 mesh, from Ted Pella), and then dried in air. Bright-field TEM experiments were conducted either on a Philips CM12 at 120 kV, or a JEOL 3011 at 300 kV.

2.4 Differential scanning calorimetry and hot-stage light microscopy

A Perkin Elmer DSC6 with Pyris Thermal Analysis System (Version 3.52) was used to examine the thermal properties of powder samples (5–10 mg). Heating and cooling rates of 10 °C min^{-1} were applied throughout this work. An isothermal holding of 1 and 5 min was programmed at the lowest and highest temperatures in the thermal cycles, respectively. Nitrogen gas was flushing the system during the DSC experiments.

A Linkham TH 1500 hot stage with a TMS 91 controller was combined with our polarized optical microscope (Nikon OptiPhot2-POL) to achieve hot-stage optical microscopy experiments.

2.5 Electron diffraction

Selected area electron diffraction experiments were conducted on either a Philips CM12 at 120 kV, or a JEOL 3011 at 300 kV. Thin thermally evaporated gold films were adopted as diffraction standard. Au (111) planes (0.2355 nm) were generally used as a calibration for *d*-spacing measurements of unknowns.

2.6 Molecular simulation

Crystal structure visualization and comparison were made with Cerius[2] (Accelrys, Inc.) and Mercury 1.4.1 (Cambridge Crystallographic Data Centre) platforms. Unit cell information of different pentacene variations was obtained with single crystal X-ray diffraction experiments. Data for the determination of functionalized pentacene crystal structures were collected on either a Nonius kappaCCD or a Bruker-Nonius X8 Proteum instrument.

3. Results and discussion

3.1 Synthesis and molecular structure

The n-alkylethynyl (*n*-P) and diisopropyl alkylsilylethynyl (*n*-Si) pentacene derivatives were prepared to study the effects of alkyl group length on crystal structure as well as optical, thermal and

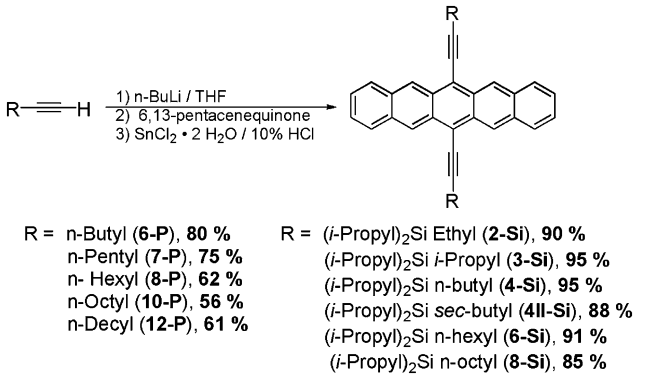

Fig. 1 The synthesis and yields of functionalized pentacenes. There were two types of pentacenes studied in this present work. Alkyl acetylene series included 6-P, 7-P, 8-P, 10-P, and 12-P, while alkylsilylethynyl series had 2-Si, 3-Si, 4-Si, 4II-Si, 6-Si, and 8-Si.

stability properties of functionalized pentacene (Fig. 1). The requisite ethynyllithium solutions were prepared by treatment of the alkyne with n-BuLi in THF, followed by addition of commercially available 6,13-pentacenequinone. After the quinone had dissolved completely, the reaction was quenched with 10% aqueous HCl / tin (II) chloride, which induced deoxygenation and yielded the desired pentacene derivatives.

Even during the workup process, the alkylethynyl pentacenes (*n*-P) proved to be poorly stable, with the decynyl and dodecynyl (10-P and 12-P) derivatives particularly prone to decomposition—in fact, the decynyl derivative 10-P was barely stable enough to obtain full characterization. The diisopropylsilyl derivatives, in contrast, were significantly more stable, soluble and easy to purify. The instability of the n-alkylethynyl pentacenes is likely due to the facile Diels–Alder reaction between unhindered alkynes and the pentacene chromophore.[30,31] Longer side chains tended to hinder crystal formation and facilitate the proper geometry conditions for Diels–Alder reaction. Thus 8-Si, 10-P, 8-P, and 7-P were found to be easier to degrade than their shorter-side-chain counterparts.

Table 1 summarizes the solubility properties of various functionalized pentacenes as compared to triethylsilylethynyl anthradithiophene (TES-ADT), a promising new candidate for high-performance organic thin film transistors.[32] TES-ADT

Table 1 The solubilities of functionalized pentacenes in hexane and THF as compared to triethylsilylethynyl anthradithiophene (TES-ADT)[a]

	Hexane	THF
6-P	<0.1%	1%
7-P	≪0.1%	0.5%
8-P	<0.1%	2.5%
10-P	≪0.1%	2.5%
12-P	1%	2.5%
2-Si	1%	5%
3-Si	0.25%	1%
4-Si	0.5%	2.5%
4II-Si	1%	1%
6-Si	1%	2.5%
8-Si	2.5%	5%
TES ADT	<0.1%	1%

[a] Two samples for each data point. The unit is mg solute per μL solvent.

Published on 12 February 2008. Downloaded by CASE WESTERN RESERVE UNIVERSITY on 30/10/2014 17:04:20.

and most of the functionalized pentacenes examined in this work had significantly higher solubility in THF than in hexane, except that 4II-Si had roughly the same solubility in both solvents. To describe and predict the extent of mixing interactions between the solutes and solvents, solubility parameters[33] offered a convenient and easy means of quantitative evaluation. Solubility parameter (δ) is defined as the square root of the cohesive energy density (CED).[33] Since the solubility parameter of hexane is 14.9 $(MPa)^{1/2}$ and that of THF is 18.6 $(MPa)^{1/2}$, the solubility parameters of most functionalized pentacenes were estimated to be around 18–19 $(MPa)^{1/2}$, if one assumed that the Gibbs free energy of mixing $\triangle G_m = \triangle H_m - T\triangle S_m$, the entropy of mixing $\triangle S_m$ was negligible, and the enthalpy of mixing $\triangle H_m = (\delta_1 - \delta_2)^2\varphi_1\varphi_2 V$ was a function of the difference in solubility parameters between solute and solvent (δ_1, δ_2; subscript "1" stands for solvent, "2" for solute), the volume fractions (φ_1, φ_2) and the volume of the mixture (V).[34]

Unlike unfunctionalized pentacene, in a good solvent such as THF, alkylsilylethynyl and alkylethynyl pentacenes exhibited rather high solubilities of 0.5–5% (solute mass in mg per solvent volume in μL), which were sufficient for potentially low-cost and large-area solution deposition processes. Alkylsilylethynyl pentacenes showed substantially higher solubilities (1–5% in THF, 0.25–2.5% in hexane) than those of their non-silicon-based counterparts with similar chain lengths (0.5–2.5% in THF, <0.1–1% in hexane), possibly because of the fractal shapes of side chains. In addition, longer side chains tended to yield better solubility for both alkylsilylethynyl and alkylethynyl pentacenes in all solvents, although there were a few exceptions such as 2-Si and 4-Si. Most of the functionalized pentacenes shown here had superior solubility to that of TES-ADT because of their larger side chains.

The temperature dependent solubilities of 3-Si, also called 6,13-bis(triisopropylsilylethynyl) (TIPS) pentacene, are presented in Table 2. The solubilities of other functionalized pentacenes were expected to undergo similar trends as the temperature increased. This information is especially useful when elevated-temperature deposition is necessary in order to fabricate films with larger grains, or to speed up the deposition rate.

3.2 UV-vis spectrocopy

The alkylsilylethynyl pentacenes demonstrated very similar UV-vis spectra in the range of 350–700 nm (Fig. 2), while the alkylethynyl series exhibited subtle changes in absorption maxima depending on alkyl chain length. Notably, both 10-P and 12-P decomposed rapidly in solution, yielding byproducts with anthracene-like chromophores (evidenced by absorptions at 380, 410 nm) (Fig. 3). Furthermore, the pentacene absorption for 12-P appears slightly blue-shifted relative to the absorptions for the other alkyl derivatives. The alkylsilylethynyl pentacenes

Table 2 The solubilities of TIPS pentacene (3-Si) in bromobenzene as a function of temperature[a]

	RT	50 °C	105 °C
TIPS pentacene	1%	2.5%	5%

[a] Three samples for each data point. The unit is mg solute per μL solvent.

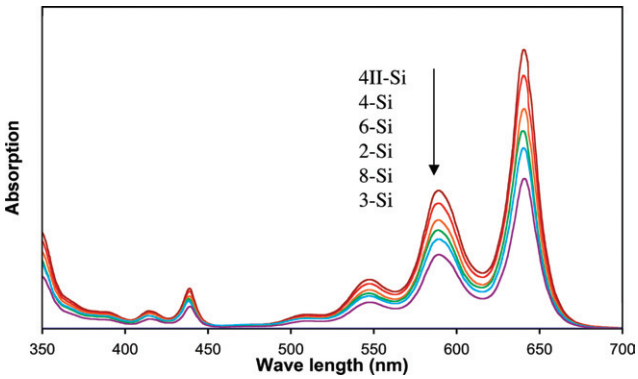

Fig. 2 UV-vis spectra of the alkylsilylethynyl pentacene series in THF solution.

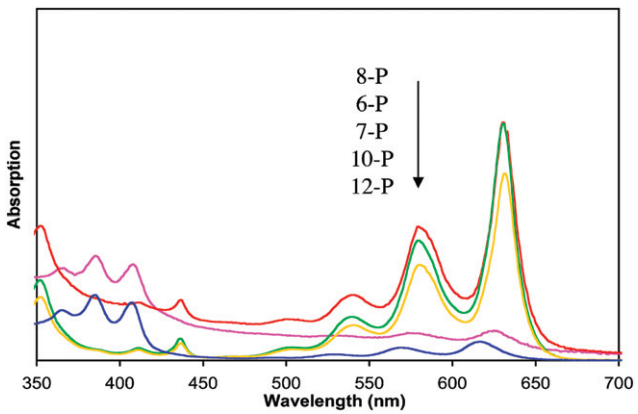

Fig. 3 UV-vis spectra of the alkyl acetylene pentacenes in THF solution.

in THF all showed a strong 645 nm peak, which started at about 660 nm (1.88 eV), the energy of the optical gap. The almost identical UV-vis absorption peaks of alkylsilylethynyl pentacenes suggested that the silyl groups effectively isolate the chromophore from the effect of variations in side chain length.

Calculated molar absorption coefficients at selected wavelengths are available as ESI.‡ The absorption intensity differences between functionalized pentacenes were partly due to the slight variation in solution concentrations, although efforts were made to keep the sample concentration around 30 mg L (in THF) for all samples in a standard 10 mm cuvette.

According to the crystal structure, the alkyne in 7-P is within 3.5 Å of one of the aromatic rings of an adjacent pentacene, which is the right distance and geometry for a Diels–Alder addition to take place in the solid state. For this reason, 7-P will be less stable during storage than other pentacene derivatives that have a crystal structure identified in this work.

3.3 Thin film morphology (optical and transmission electron microscopy)

Solution casting of functionalized pentacenes was performed on clean glass slides inside four-inch-diameter Petri dishes, either with or without cover on. This allowed rough control over the solvent evaporation rate during the film formation process. Optical micrographs of alkylsilylethynyl pentacene films are shown in Fig. 4. Covered drying turned out to be not always

 This journal is © The Royal Society of Chemistry 2008

Published on 12 February 2008. Downloaded by CASE WESTERN RESERVE UNIVERSITY on 30/10/2014 17:04:20.

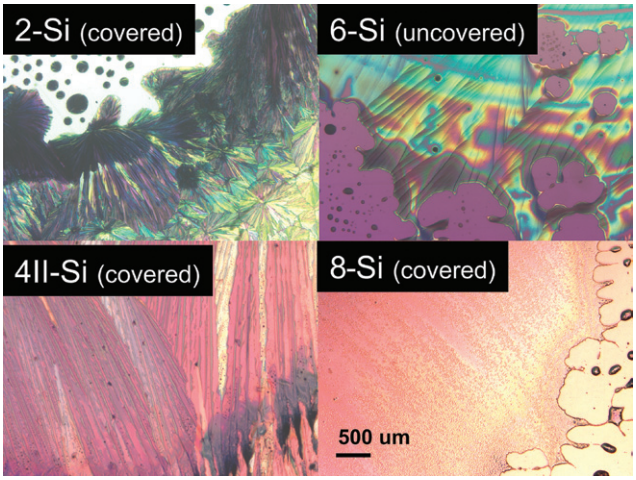

Fig. 4 Optical micrographs of solution-cast films of alkylsilylethynyl pentacenes. Films were cast from 0.1% wt. THF solutions.

advantageous, since the molecules were kept in solution (in air) for long enough that they degraded and formed non-birefringent amorphous-looking droplets.

Both bright-field TEM and optical microscopy data demonstrated that crystalline domain sizes in 4-Si, 4II-Si, and 6-Si were generally larger than those of 2-Si and 8-Si. In fact, unlike other samples in Fig. 4, the 8-Si films were barely birefringent under the polarized light microscope. Our available results suggested that too long ($\geq$8) or too short ($\leq$2) a side group impedes crystallization of these pentacene derivatives.

Optical images of solution-cast alkylethynyl pentacenes also illustrated the effect of evaporation rate on thin film morphology (as shown in uncovered and covered 12-P in Fig. 5). Uncovered 12-P films, although less uniform, exhibited significantly greater crystal sizes than covered 12-P films. The films of 10-P assumed non-birefringent droplet shapes, again supporting their quick degradation after synthesis.

X-Ray and electron diffraction experiments on these samples generally agreed with birefringence observations in polarized light microscopy.

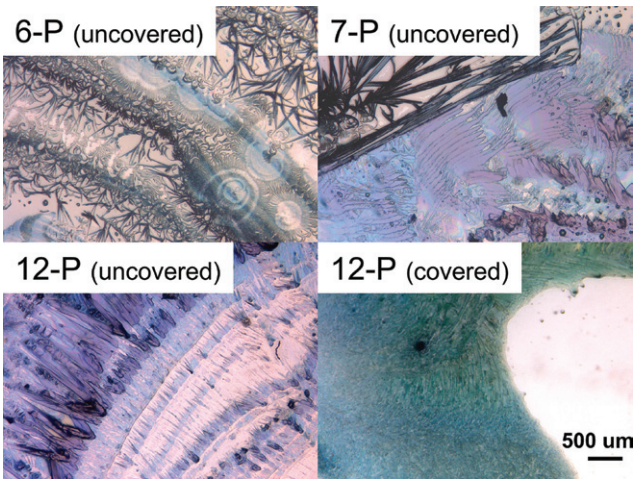

Fig. 5 Optical micrographs of solution-cast films of alkylethynyl pentacenes. Films were cast from 0.1% wt. toluene solutions.

In practice, the alkylethynyl pentacenes degraded much faster than their silicon-based counterparts both in solution and in the solid state, as observed from either a color change (blue to yellow) in solution, or birefringence loss in solution-cast films. Thus, in general, higher evaporation rates were needed for the alkylethynyl derivatives in order to generate crystalline films. Uncovered drying usually yielded more uniform and non-degraded films than covered drying in the case of alkylethynyl pentacenes, but still, their chemical stability, film coverage and crystalline domain sizes (Fig. 5) were poor when compared to the alkylsilylethynyl series (Fig. 4).

Depending upon the vacuum deposition conditions such as substrate temperature, chamber pressure, and growth rate, the crystalline domain sizes of pentacene films were generally smaller than 10 μm.[35–38] The side-group modified pentacenes shown in this work, however, can exhibit domain sizes up to millimeter or centimeter dimensions, with relatively consistent morphology, which are very desirable in order to fabricate large-area low-cost organic electronic devices. Issues on uniform coverage, and consistent crystal orientation will need to be taken into consideration in order to further improve their performance and reduce their performance variation.

3.4 Thermal properties by differential scanning calorimetry and hot-stage light microscopy

DSC of the two pentacene series showed systematic variations of thermal properties depending upon the choice of side group, and thermal stability of the silicon-based (alkylsilylethynyl) pentacenes were by far superior than the non-silicon-based (alkylethynyl) derivatives (Fig. 6 and 7). A table of phase transition temperatures and corresponding enthalpies is given in the ESI.‡

For the alkylethynyl series, degradation temperatures were so low (around 120–150 °C as indicated by the exothermic peaks upon heating) that endothermic melting transitions could be hardly seen except in the case of 12-P (Fig. 7). The melting and degradation transitions in 12-P almost overlapped with each other, so that the exothermic peak at 132 °C closely followed the endothermic transition at 128 °C. In addition, increasing length of the alkyl side groups from 6-P, 7-P, to 8-P seemed to correlate well with the decreased degradation temperature. It was expected that the longer linear side chains tended to decrease

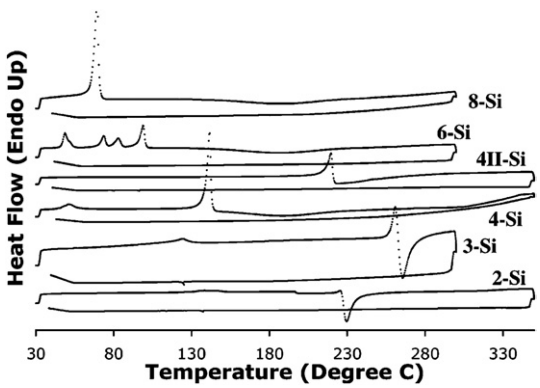

Fig. 6 Differential scanning calorimetry (DSC) of the alkylsilylethynyl pentacenes. The heating started at 30 °C, and ended at 300 or 350 °C before cooling back to 40 °C.

Published on 12 February 2008. Downloaded by CASE WESTERN RESERVE UNIVERSITY on 30/10/2014 17:04:20.

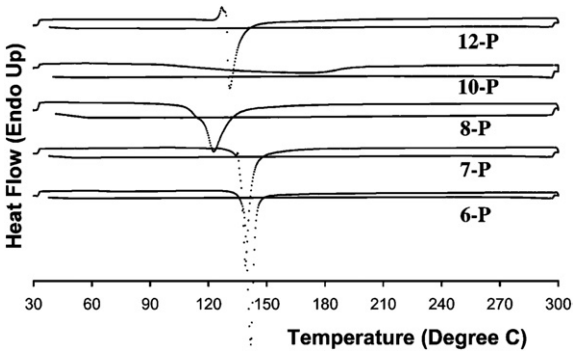

Fig. 7 DSC of the alkyl acetylene pentacenes. The heating started at 30 °C, and ended at 300 °C before cooling back to 40 °C.

the strength of the interaction between the aromatic portions of these pentacenes, making crystalline packing more difficult and thus reducing the thermal stability of the molecules. The degradation point of 8-P (123 °C) was found to be 19 °C lower than that of 6-P (142 °C) because of this side chain length effect.

The addition of silicon-based substituents to the system improved the thermal stability dramatically as in 2-Si, 3-Si, and 4II-Si (melting points: 226 °C, 263 °C, and 220 °C, respectively), although too long a linear alkyl substituent could also promote melting and for this reason the melting temperatures of 8-Si, 6-Si, and 4-Si were rather low (68 °C, 51 °C, and 142 °C) (Fig. 6). Furthermore, 3-Si, 4-Si, and 6-Si even demonstrated one or more structure changes upon heating. In the case of 3-Si, also known as 6,13-bis(triisopropylsilylethnyl) pentacene (TIPS pentacene), the sub-melting endothermic peak was caused by a well-characterized solid-to-solid structural phase transition, accompanied with characteristic cracking and facetting.[39] For 6-Si, the three endothermic transitions below the melting point suggested the possibility of thermotropic liquid crystalline phases. Although hot-stage optical microscopy demonstrated melting and recrystallization of 6-Si films upon heating and cooling, clear evidence of the exact nature of mesophases present has yet to be conclusively identified. In the cases of all alkylsilylethynyl pentacenes, as long as the temperature of DSC is not taken above 170 °C, their melting transitions are reversible according to DSC experiments. The broad exothermic transition centered at 185 °C for 8-Si, 6-Si and 4-Si likely corresponds to Diels–Alder reaction between alkyne substituents and pentacene chromophores in the melt[30]—for those compounds that melt above this temperature, this decomposition occurs immediately upon melting, due to the ability of molecules in the melt to adopt the correct geometric orientation necessary for this reaction to occur.

The melting temperature in the Si-based system correlates strongly with the amount of π-overlap observed in the crystals (also discussed below in section 3.6). 3-Si possesses the strongest π-overlap, and exhibits the highest melting point. 2-Si and 4-Si have significantly less π-overlap, and thus melt at significantly lower temperatures; there is no π-overlap seen in the crystals of 6-Si and 8-Si, leading to exceptionally low thermal stabilities for these compounds.

Compared to unsubstituted pentacene (melting point >300 °C), all the functionalized pentacenes showed less thermal stability. The thermal stabilities of alkylethynyl pentacenes were reduced by more than 160 °C, upon the addition of side groups. In some of the alkylsilylethynyl pentacenes (3-Si, 4II-Si, and 2-Si), however, the differences were successfully minimized to 40–90 °C. Further information on the chemical stability of functionalized pentacenes upon heating could be obtained by employing thermogravimetric analysis (TGA), which was not pursued in this study.

3.5 Electron diffraction and crystallinity

Selected area electron diffraction patterns revealed that the alkylsilylethynyl pentacenes generally exhibited higher crystallinity and more single-crystal features than the alkylethynyl pentacenes. Using a 5 μm diffraction aperture, it was relatively easy to obtain sharp single-crystal patterns with 6-Si, and 4-Si (Fig. 8), and arcs with 2-Si or 8-Si (Fig. 9 and Fig. 10 left). For 3-Si, a single-crystal [001] pattern was frequently observed as evidence of the edge-on orientation of acene rings on the substrate.[39] However, with n-alkylethynyl pentacenes, broad rings were usually seen under the same conditions. A representative ring pattern of 12-P is shown in Fig. 10 (right). In addition, silicon-based pentacenes generally had distinctive facetting in bright-field TEM images, whereas their n-alkylethynyl counterparts often adopted an irregular appearance. These results

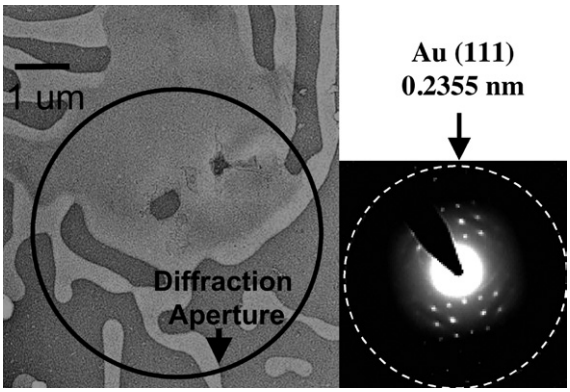

Fig. 8 Representative electron micrograph and corresponding diffraction pattern for 6-Si thin film. Sample prepared with THF solution (0.1% wt.) on amorphous carbon substrate.

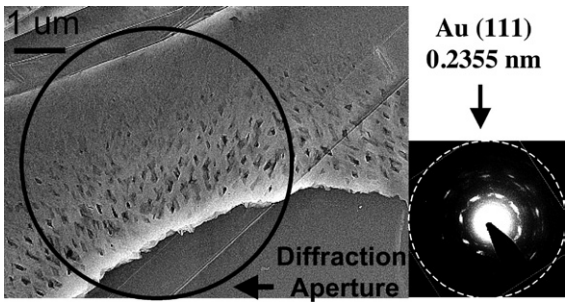

Fig. 9 Representative electron micrograph and corresponding electron diffraction pattern (aperture as shown in the TEM image) for 2-Si films. The dotted ring in the diffraction pattern was the spacing for Au (111) (0.2355 nm). Sample prepared with THF solution (0.1% wt.) on amorphous carbon substrate.

 This journal is © The Royal Society of Chemistry 2008

Published on 12 February 2008. Downloaded by CASE WESTERN RESERVE UNIVERSITY on 30/10/2014 17:04:20.

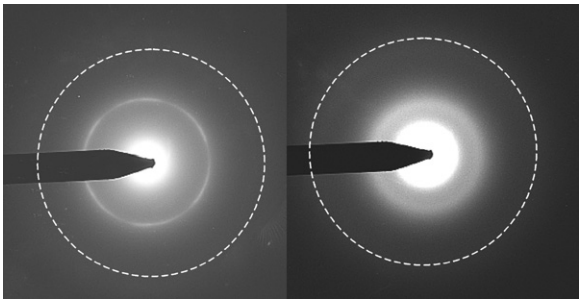

Fig. 10 Representative electron diffraction patterns for 8-Si (left) and 12-P (right). The dotted rings in diffraction patterns were the spacing for Au (111) (0.2355 nm). Sample prepared with THF solution (0.1% wt.) on amorphous carbon substrate.

suggest that silyl substituents enhance the formation of crystalline films.

According to the electron pattern and fading observed in electron diffraction experiments with the same imaging conditions, a comparison of crystallinity could be made between samples. The crystallinity sequence was determined to be 3-Si > 6-Si, 4-Si, 4II-Si > 2-Si > 8-Si. This agreed well with the previous findings in the literature that an intermediate alkyl length can promote crystal packing and π–π interactions.[15,16,40] In the case of alkylsilylethynyl pentacene, an alkyl chain size of 3–6 carbons was found to be optimal for maximizing crystallinity.

Because of the alkyl side chains on each acene unit, the aromatic content in these functionalized pentacenes is substantially lower than that of plain pentacene. The critical electron dose of beam damage for 3-Si was experimentally determined to be 0.045 C cm^{-2} at 300 kV,[34] which was several times lower than that of pentacene (0.2 C cm^{-2} at 100 kV).[41] As the electron beam resistivity of organic crystals is closely related to their thermal stability [42,43] and 3-Si had the best thermal stability (melting and degradation temperature around 260 °C) among the alkylsilylethynyl and alkylethynyl pentacenes, the other functionalized pentacenes examined in this work were expected to have much lower electron critical doses and shorter lifetimes under the transmission electron microscope than those of 3-Si and straight pentacene.

3.6 Crystal packing as a function of systematically varied side chains

Although the general packing arrangement of pentacene molecules in these two classes of compounds did not change in a monotonic fashion with increasing length of alkyl chain, the intermolecular interactions did follow a general trend across both of these systems. First of all, in contrast to the "herringbone" arrangement of acene cores in neat pentacene crystals, most of the functionalized pentacenes in this work adopted a co-planar arrangement, with many exhibiting regular π–π interactions (Fig. 11). In the cases with shorter alkyl chains (ethyl, isopropyl, butyl) the pentacene units adopted strongly π-stacked arrangements, with contacts as close as 3.39 Å (as compared with 6.27 Å in unsubstituted pentacene) between carbon atoms in adjacent pentacene units (Fig. 11 shows interaction between acene nearest neighbors in the solid state).[44] As the length of the aliphatic chain is increased beyond 4 carbon atoms (*e.g.* 6-Si, 7-P), interactions between the long alkyl chain and the

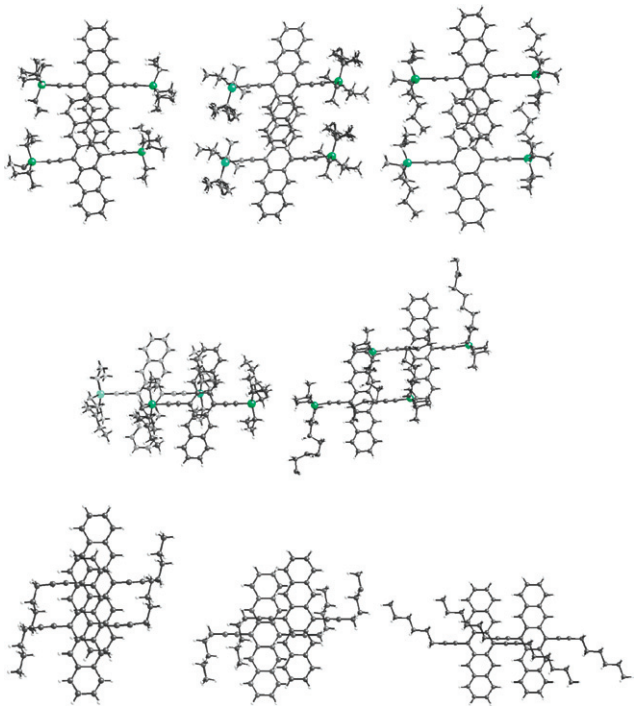

Fig. 11 Crystal packing of the functionalized pentacene unit cells. Top row: 2-Si, 3-Si, and 4-Si; second row: 6-Si and 8-Si; third row: 6-P, 7-P, and 8-P. In contrast to the regular π–π stacking in functionalized pentacenes studied in this work, unsubstituted pentacene has a "herringbone" arrangement between acenes.

pentacene chromophore begin to dominate the packing, and π-stacking interactions are lost completely. Further increases in alkyl chain length (8-Si, 8-P) only serve to more completely insulate the pentacene unit from adjacent pentacene chromophores, making them poor choices for applications in electronic devices. Just as with the substituted oligothiophenes, in both the alkylethynyl and alkylsilylethynyl pentacenes the optimum chain length appears to lie between C2 and C5.

The available lattice parameters for the two series of functionalized pentacenes are tabulated with their unit cell symmetry information in Table 3, compared to two common polymorphs of pentacene (Pentacene 1 is a common bulk phase[28] and Pentacene 2 was a thin film phase[45]). There were no values available for 10-P and 12-P, possibly due to the fact that the long linear chains in those molecules made crystal packing rather difficult and the fact that 10-P degraded readily upon synthesis.

3.7 Electrical properties

Thin-film transistors were constructed from several of the derivatives reported in this work, although so far only 2-Si and 3-Si exhibited field effects. Since we did not apply self-assembled monolayers to pre-treat the silicon dioxide substrate and did not optimize the channel width/length based on the specific film morphology, better device performances of these materials are likely to be observed with more thorough electrical characterization in the future.

As with the previously reported 8-P,[46] most of the alkylethynyl pentacenes (except 6-P) did not yield thin films of high enough

Published on 12 February 2008. Downloaded by CASE WESTERN RESERVE UNIVERSITY on 30/10/2014 17:04:20.

Table 3 Crystal structures of the pentacene derivatives with systematically changed side chains, as compared to two pentacene polymorphs (Pentacene 1 is a common bulk phase: Holmes *et al.*;[28] Pentacene 2 is a thin film phase: Drummy *et al.*[45]). The units of lattice parameters *a*, *b*, *c* are angstroms

Material	Crystal system	Space group	*a*	*b*	*c*	*α*	*β*	*γ*
6-P	Monoclinic	*P*21/*C*	19.8513	5.3006	22.6989	90	93.5526	90
7-P	Monoclinic	*P*21/*N*	12.3212	5.142	20.803	90	101.1599	90
8-P	Triclinic	$P\bar{1}$	6.6368	8.3446	13.7421	105.5261	100.2523	92.736
2-Si	Triclinic	$P\bar{1}$	10.6177	13.6171	14.0829	75.154	73.915	71.123
3-Si	Triclinic	$P\bar{1}$	7.55	7.73	16.76	89.5	78.7	84
4-Si	Monoclinic	*P*21/*C*	8.884	22.324	10.797	90	110.146	90
6-Si	Orthorhombic	*PBCA*	10.3715	15.4649	27.5066	90	90	90
8-Si	Triclinic	$P\bar{1}$	8.8577	11.129	12.5975	101.9194	93.8211	101.2905
Pentacene 1	Triclinic	$P\bar{1}$	6.28	7.71	14.44	76.75	88.01	84.52
Pentacene 2	Orthorhombic	N/A	5.9 ± 0.2	7.4 ± 0.2	30.0 ± 0.8	90	90	90

quality for transistor studies. Of the alkylsilylethynyl derivatives, 3-Si has well known solution-processed transistor properties comparable to, or even superior to, pentacene in some cases, which is in part made possible by the strong two-dimensional π-stacking observed in this material.[29,34,39,47–52] In contrast, neither 6-Si nor 8-Si exhibit any close contacts between aromatic rings in the solid state, and the thin films of these two materials were either not uniform enough, or suffering with degradation on the silicon wafer (evidenced by the birefringence loss in polarized light microscopy). All of 2-Si, 4-Si, and 4II-Si were found to be chemically stable upon solution casting, forming well-covered and textured thin films on silicon wafers. In the future, it is expected that a reasonable compromise between the thermal issues observed in 3-Si and high mobility may be found by designing proper side chains to provide minimal mechanical cracking, acceptable thermal stability, and decent electrical properties for various device applications.

4. Conclusions

We found that crystal packing, optical and thermal properties changed in a systematic way with increasing lengths of alkyl groups substituted on pentacene chromophores. The optimum alkyl chain in these systems was between 2 and 5, with hexyl chains or longer leading to complete elimination of desirable π-stacking interactions. The Si-based series was much more thermally and chemically stable, as well as more crystalline than the non-Si-based ones according to DSC and electron diffraction experiments.

Acknowledgements

The authors would like to thank the Office of Naval Research and the National Science Foundation for financial support (DMR-0084304 and DMR-6518079). TEM studies were conducted at the Electron Microbeam Analysis Laboratory (EMAL) at the University of Michigan at Ann Arbor, with assistance from the lab managers, Dr Carl Henderson, Dr John Mansfield, and Dr Kai Sun. J.C. appreciated constructive discussions with Professor Adam Matzger in the Chemistry Department at the University of Michigan. The Philips CM12 scanning transmission TEM used in this work was obtained from NSF under the grant #EAR-87-08276, and the JEOL3011 was obtained from the support of NSF grant #DMR-0315633.

References

1 C. W. Tang, *Appl. Phys. Lett.*, 1986, **48**, 183.
2 C. W. Tang and S. A. VanSlyke, *Appl. Phys. Lett.*, 1987, **51**, 913.
3 G. Horowitz, D. Fichou, X. Peng, Z. Xu and F. Garnier, *Solid State Commun.*, 1989, **72**, 381.
4 D. Wohrle and D. Meissner, *Adv. Mater.*, 1991, **3**, 129.
5 F. Garnier, F. Deloffre, G. Horowitz and R. Hajlaoui, *Synth. Met.*, 1993, **55–57**, 4747.
6 A. Dodabalapur, L. Torsi and H. E. Katz, *Science*, 1995, **268**, 270.
7 F. Garnier, *Curr. Opin. Solid State Mater. Sci.*, 1997, **2**, 455.
8 F. Garnier, G. Horowitz, D. Fichou and A. Yassar, *Supramol. Sci.*, 1997, **4**, 155.
9 P. K. H. Ho, J.-S. Kim, J. H. Burroughes, H. Becker, S. F. Y. Li, T. M. Brown, F. Cacialli and R. H. Friend, *Nature*, 2000, **404**, 481.
10 C. D. Dimitrakopoulos and P. R. L. Malenfant, *Adv. Mater.*, 2002, **14**, 99.
11 S. R. Forrest, *Nature*, 2004, **428**, 911.
12 M. Pope and C. E. Swenberg, *Electronic processes in organic crystals and polymers*, Oxford University Press, Oxford, UK, 2nd edn, 1999.
13 H. Yanagi, Y. Araki, T. Ohara, S. Hotta, M. Ichikawa and Y. Taniguchi, *Adv. Funct. Mater.*, 2003, **13**, 767.
14 C. Videlot, J. Ackermann, P. Blanchard, J. M. Raimundo, P. Frere, M. Allain, R. de Bettignies, E. Levillain and J. Roncali, *Adv. Mater.*, 2003, **15**, 306.
15 M. Halik, H. Klauk, U. Zschieschang, G. Schmid, W. Radlik, S. Ponomarenko, S. Kirchmeyer and W. Weber, *J. Appl. Phys.*, 2003, **93**, 2977.
16 M. Halik, H. Klauk, U. Zschieschang, G. Schmid, S. Ponomarenko, S. Kirchmeyer and W. Weber, *Adv. Mater.*, 2003, **15**, 917.
17 K. Ito, T. Suzuki, Y. Sakamoto, D. Kubota, Y. Inoue, F. Sato and S. Tokito, *Angew. Chem., Int. Ed.*, 2003, **42**, 1159.
18 H. Klauk, D. J. Gundlach, J. A. Nichols and T. N. Jackson, *IEEE Trans. Electron Devices*, 1999, **46**, 1258.
19 C. D. Dimitrakopoulos, A. R. Brown and A. Pomp, *J. Appl. Phys.*, 1996, **80**, 2501.
20 M. G. Kane, J. Campi, M. S. Hammond, F. P. Cuomo, B. Greening, C. D. Sheraw, J. A. Nichols, D. J. Gundlach, J. R. Huang, C. C. Kuo, L. Jia, H. Klauk and T. N. Jackson, *IEEE Electron Device Lett.*, 2000, **21**, 534.
21 H. Klauk, D. J. Gundlach and T. N. Jackson, *IEEE Electron Device Lett.*, 1999, **20**, 289.
22 J. A. Rogers, Z. Bao, K. Baldwin, A. Dodabalapur, B. Crone, V. R. Raju, V. Kuck, H. Katz, K. Amundson, J. Ewing and P. Drzaic, *Proc. Natl. Acad. Sci. U. S. A.*, 2001, **98**, 4835.
23 P. Mach, S. J. Rodrigues, R. Nortrup, P. Wiltzius and J. A. Rogers, *Appl. Phys. Lett.*, 2001, **78**, 3592.
24 C. D. Sheraw, L. Zhou, J. R. Huang, D. J. Gundlach, T. N. Jackson, M. G. Kane, I. G. Hill, M. S. Hammond, J. Campi, B. K. Greening, J. Franci and J. West, *Appl. Phys. Lett.*, 2002, **80**, 1088.
25 S. F. Nelson, Y.-Y. Lin, D. J. Gundlach and T. N. Jackson, *Appl. Phys. Lett.*, 1998, **72**, 1854.

 This journal is © The Royal Society of Chemistry 2008

Published on 12 February 2008. Downloaded by CASE WESTERN RESERVE UNIVERSITY on 30/10/2014 17:04:20.

26 Y. Y. Lin, D. J. Gundlach, S. F. Nelson and T. N. Jackson, *IEEE Electron Device Lett.*, 1997, **18**, 606.
27 K. Shankar and T. N. Jackson, *J. Mater. Res.*, 2004, **19**, 2003.
28 D. Holmes, S. Kumaraswamy, A. J. Matzger and K. P. C. Vollhardt, *Chem.–Eur. J.*, 1999, **5**, 3399.
29 J. Chen, C. K. Tee, C. Shaw, M. Shtein, D. C. Martin and J. E. Anthony, *J. Polym. Sci., Part B: Polym. Phys.*, 2006, **44**, 3631.
30 M. M. Payne, S. A. Odom, S. R. Parkin and J. E. Anthony, *Org. Lett.*, 2004, **6**, 3325.
31 Y. Kim, J. E. Whitten and T. M. Swager, *J. Am. Chem. Soc.*, 2005, **127**, 12122.
32 K. C. Dickey, J. E. Anthony and Y. L. Loo, *Adv. Mater.*, 2006, **18**, 1721.
33 A. F. M. Barton, *CRC Handbook of solubility parameters and other cohesion parameters*, CRC, Boca Raton, FL, 1st edn, 1983.
34 J. Chen, J. E. Anthony and D. C. Martin, *J. Mater. Res.*, 2007, **22**, 1701.
35 M. Shtein, J. Mapel, J. B. Benziger and S. R. Forrest, *Appl. Phys. Lett.*, 2002, **81**, 268.
36 A. Bolognesi, M. Berliocchi, M. Manenti, A. D. Carlo, P. Lugli, K. Lmimouni and C. Dufour, *IEEE Trans. Electron Devices*, 2004, **51**, 1997.
37 A. D. Carlo, F. Piacenza, A. Bolognesi, B. Stadlober and H. Maresch, *Appl. Phys. Lett.*, 2005, **86**, 263501.
38 D. Knipp, R. A. Street, A. Volkel and J. Ho, *J. Appl. Phys.*, 2003, **93**, 347.
39 J. Chen, J. E. Anthony and D. C. Martin, *J. Phys. Chem. B*, 2006, **110**, 16397.
40 H. E. Katz, Z. Bao and S. Gliat, *Acc. Chem. Res.*, 2001, **34**, 359.
41 J. P. Martinez, D. Locateli, J. L. Balladore and J. Trinquier, *Ultramicroscopy*, 1982, **8**, 437.
42 S. Kumar and W. W. Adams, *Polymer*, 1990, **31**, 15.
43 D. C. Martin and E. L. Thomas, *Polymer*, 1995, **36**, 1743.
44 J. E. Anthony, J. S. Brooks, D. L. Eaton and S. R. Parkin, *J. Am. Chem. Soc.*, 2001, **123**, 9482.
45 L. F. Drummy and D. C. Martin, *Adv. Mater.*, 2005, **17**, 903.
46 C. D. Sheraw, T. N. Jackson, D. L. Eaton and J. E. Anthony, *Adv. Mater.*, 2003, **15**, 2009.
47 S. K. Park, T. N. Jackson, J. E. Anthony and D. A. Mourey, *Appl. Phys. Lett.*, 2007, **91**, 063514.
48 J. G. Park, R. Vasic, J. S. Brooks and J. E. Anthony, *J. Appl. Phys.*, 2006, **100**, 044511.
49 J. G. Park, R. Vasic, J. S. Brooks and J. E. Anthony, *J. Low Temp. Phys.*, 2007.
50 W. H. Lee, D. H. Kim, Y. Jang, J. H. Cho, M. Hwang, Y. D. Park, Y. H. Kim, J. I. Han and K. Cho, *Appl. Phys. Lett.*, 2007, **90**, 132106.
51 D. H. Kim, D. Y. Lee, H. S. Lee, W. H. Lee, Y. H. Kim, J. I. Han and K. Cho, *Adv. Mater.*, 2007, **19**, 678.
52 J. Chen, *Structure, processing, and properties of the organic molecular semiconductor triisopropylsilylethnyl (TIPS) pentacene*, PhD Dissertation, University of Michigan at Ann Arbor, 2006.